Heteropolyacids@Silica Heterogeneous Catalysts to Produce Solketal from Glycerol Acetalization

Catarina N. Dias , Isabel C.M.S. Santos-Vieira , Carlos R. Gomes , Fátima Mirante * , Salete S. Balula *

Posted Date: 26 March 2024

doi: 10.20944/preprints202403.1537.v1

Keywords: acetalization; solketal; heteropolyacids; mesoporous silica

Article

Heteropolyacids@Silica Heterogeneous Catalysts to Produce Solketal from Glycerol Acetalization

Catarina N. Dias [1], Isabel C.M.S. Santos-Vieira, [2] Carlos R. Gomes [3], Fátima Mirante [1,*] and Salete S. Balula [1,*]

[1] LAQV/REQUIMTE & Department of Chemistry and Biochemistry, Faculty of Sciences, University of Porto, 4169-007 Porto, Portugal
[2] CICECO—Aveiro Institute of Materials, Department of Chemistry, University of Aveiro, 3810-193 Aveiro, Portugal
[3] CIMAR/CIIMAR – Centro Interdisciplinar de Investigação Marinha e Ambiental & Faculdade de Ciências, Universidade do Porto, 4169-007 Porto, Portugal; crgomes@fc.up.pt (C.R.G.)
* Correspondence: fatimaisabelmirante@gmail.com (F.M.); sbalula@fc.up.pt (S.S.B.)

Abstract: The composites of heteropolyacids (H_3PW_{12}, H_3PMo_{12}) incorporated into amine-functionalized silica materials, were used for the first time as heterogeneous catalysts in the valorisation of glycerol (a large waste from biodiesel industry) by acetalization reaction with acetone. The polyoxotungstate catalyst H_3PW_{12}@*Aptes*SBA-15 presented higher catalytic efficiency than the phosphomolybdate, with 97% of conversion with 97% of solketal selectivity, after 60 min at 25 °C, or 91% of glycerol conversion and the same selectivity, after 5 min, performing the reaction at 60 ºC. A relation of catalytic performance and acidity of the catalyst is here presented. Furthermore, the stability of the solid catalyst was investigated and discussed.

Keywords: acetalization; solketal; heteropolyacids; mesoporous silica

1. Introduction

The use of fossil fuels as an energetic resource has led to increased environmental concerns, due to the emission of greenhouse gases, known to be one of the main contributors to climate change [1,2]. The growing environmental awareness has led to the implementation of legislation, predicting the decrease of fossil fuel consumption. Interest in new energy alternatives has peaked, raising particular attention for biomass and its application in fuel formulation [3].

Biodiesel production has increased in recent years, leading to a large amount of glycerol waste, a known co-product obtained in biodiesel formulation. Biodiesel production results in the co-production of glycerol in 10%, with purity ranging 50-55% [1]. The market is unable to utilize this excess of glycerol, since it cannot be utilized in its crude state and the purification process can become extremely costly, when performed at a large scale [4,5]. However, it is essential to transform glycerol into compounds of high commercial value, due to its outstanding potential as a raw material for generation of value-added products [3,6]. Various catalytic reactions for glycerol valorization have been studied, with acetalization gaining exponential interest, since the products obtained from this reaction can contribute for a Circular Economy Model associated to the biodiesel industry [1]. Acetalization of glycerol in the presence of carbonyl compounds (aldehydes or ketones) yields solketal (2,2-dimethyl-1,3-dioxolone-4-methanol), acetal (1,3-dioxan-5-ol) and water. Solketal is a promising compound, thanks to its extraordinary performance as an oxygenated fuel additive, improving fuel characteristics [5]. Its production can be favored by using acid catalysts, such as Brönsted or Lewis acids [6,7]. Keggin heteropolyacids (HPAs) are an attractive group of solid acid catalysts, highly active in oxidative processes or acid-catalyzed reactions, thanks to the extensive sum of active sites available in their surface [8–10]. The most studied HPAs are the phosphotungstic acid ($H_3PW_{12}O_{40}$, abbreviated as H_3PW_{12}), phosphomolybdic acid ($H_3PMo_{12}O_{40}$, abbreviated as H_3PMo_{12}) and

 doi:10.20944/preprints202403.1537.v1

silicotungstic acid ($H_4SiW_{12}O_{40}$, abbreviated as H_4SiW_{12}) [11]. Da Silva et al. studied the influence of different HPAs in glycerol conversion, in the presence of propanone [12]. In particular, $H_3PW_{12}O_{40}$ distinguished itself, obtaining higher conversions (83%, at room temperature after 2 h) than the other heteropolyacids [12]. Similarly, Julião et al. reported HPAs activity in acetalization reactions at room temperature, observing the following behaviour: PW_{12} (99.2%) > PMo_{12} (91.4%) > SiW_{12} (90.7%), after only 5 minutes of reaction [13]. Da Silva et al. demonstrated that the $Sn_2SiW_{12}O_{40}$ salt is more active (> 99 % conversion, after 1 h of reaction, at room temperature) than its tin (II) chloride salt precursor, as well as other heteropoly salts and solid supported catalysts [4].

Despite the efficiency that HPAs have demonstrated in acetalization reactions, the recycle capacity of these catalysts is rarely reported. This type of catalyst is soluble in polar solvents, a feature that hinders catalyst recovery and reuse, leading to an added inconvenience in continuous solketal production [14]. One feasible method to solve this problem is to support HPAs on support inactive materials, such as mesoporous silicas [15], MOFs [16], active carbon [17] or ion-exchange resins [18]. In particular, mesoporous silica-based catalysts have acquired attention, due to the stability of these supports and the high diffusion due to their pore tunability [19]. Chen et al. investigated the catalytic efficiency of a cesium salt of phosphotungstate ($Cs_{2.5}$), in bulk and supported in KIT-6 silica [20]. Both catalysts obtained similar conversions, with the reaction time being shortened (from 60 minutes to 15 minutes), when using the supported material. Furthermore, the $Cs_{2.5}$/KIT-6 catalyst was reused for three cycles, with no loss of activity [20]. Castanheiro reported the use of silica supported HPAs in the acetalization of glycerol with citral, where H_3PW_{12}@KIT-6 showed high stability after five consecutive cycles [21].

In this work, homogeneous HPAs and heterogeneous HPAs, supported in mesoporous functionalized SBA-15 silica, were applied in acetalization reaction of glycerol with acetone. Two different heterogeneous catalysts were prepared by immobilizing H_3PW_{12} and H_3PMo_{12} onto the amine-functionalized silica support (*Aptes*SBA-15). The influence of various reaction parameters, such as catalyst acidity and temperature were analyzed to improve the conversion and selectivity of solketal as the product of interest. Catalyst stability was investigated.

2. Results and Discussion

2.1. Catalysts Characterization

The composite materials were prepared by an impregnation method, through the incorporation of heteropolyacids (HPAs) in the previously amine-functionalized SBA-15 support (*Aptes*SBA-15). The support, functionalized support and composites were characterized by several techniques including elemental analysis, zeta potential (ζ), FTIR-ATR, powder XRD, nitrogen adsorption-desorption isotherms, ICP-OES and SEM/EDS.

The SBA-15 and *Aptes*SBA-15 supports presented zeta potentials of -17.5 mV and 29.3 mV, respectively. These values were in agreement with the literature, in which the change of signal (from negative to positive) has been reported, occurring due to the successful functionalization of the amino groups on the support surface [22]. Elemental analysis of *Aptes*SBA-15 further confirmed the surface functionalization, obtaining 2.4% of nitrogen, which corresponded to 1.1 mmol of *Aptes* per g of material. The FTIR-ATR spectra of the prepared materials is shown in Figure 1A, where the characteristic vibration modes of the silica support can be observed in the region 1100-400 cm^{-1}, namely for the ν_{as} (Si-O-Si), ν_s (Si-O-Si) and δ (Si-O-Si) vibrations [23]. The presence of amino groups in 1200-1000 cm^{-1} region was unable to be identified due to overlap with the siliceous support vibration modes [24]. The incorporation of HPAs in the prepared composites was confirmed through the identification of the vibration bands at 1000-960 cm^{-1} and 800-760 cm^{-1}, corresponding to the ν_{as} (M=O_d) and ν_{as} (M-O_c-M) vibration modes, respectively [25]. Furthermore, the incorporation of HPAs in the composites was confirmed through ICP-OES analysis, where loadings of 159 and 188 μmol of HPA per g of composite were obtained, for H_3PW_{12}@*Aptes*SBA-15 and H_3PMo_{12}@*Aptes*SBA-15, respectively.

 doi:10.20944/preprints202403.1537.v1

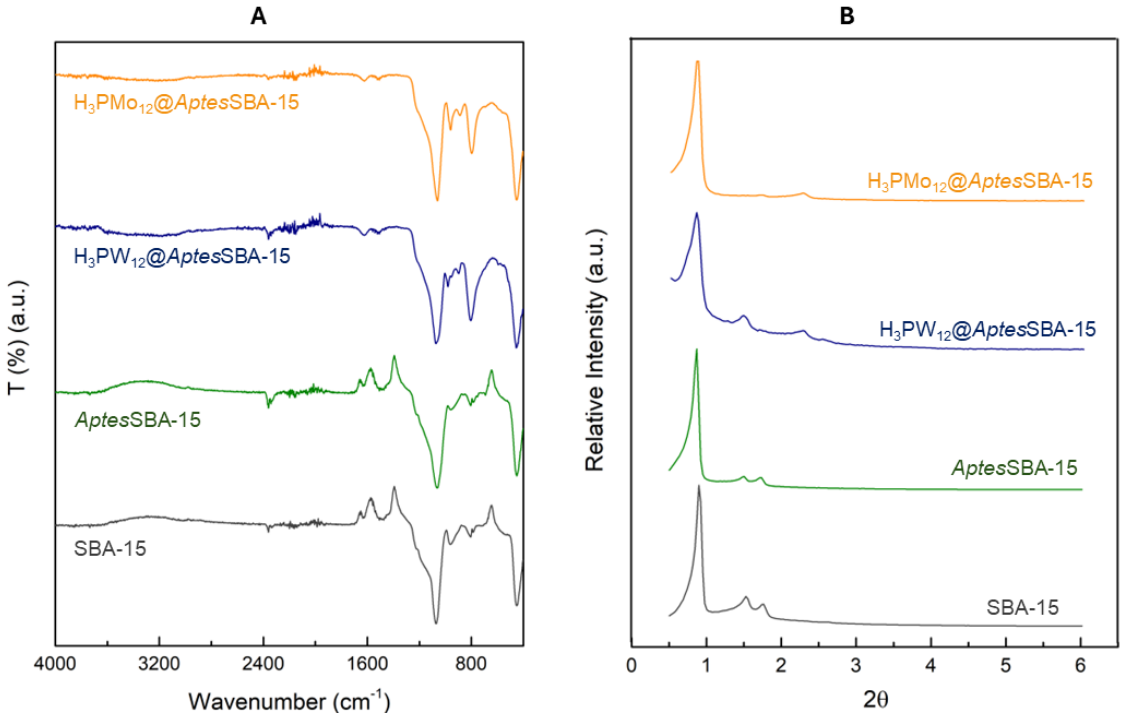

Figure 1. (A) FTIR spectra of SBA-15, *Aptes*SBA-15, H_3PW_{12}@*Aptes*SBA-15 and H_3PMo_{12}@*Aptes*SBA-15. **(B)** Powder XRD patterns for SBA-15, *Aptes*SBA-15, H_3PW_{12}@*Aptes*SBA-15 and H_3PMo_{12}@*Aptes*SBA-15.

The XRD patterns of the materials are depicted in Figure 1B. The SBA-15 support has a hexagonal structure, with three characteristic well-resolved peaks in the low-angle area. The strong peak around 1° can be attributed to the (100) plane and the two weak peaks around 1.5° and 1.8° to the (110) and (200) planes [26]. The functionalized surface of SBA-15 did not compromise the structure and crystallinity of the material, since *Aptes*SBA-15 exhibited the same peaks as the non-functionalized material. In the composites, the peaks of the (110) and (200) reflections were shifted to higher 2θ, as reported before in the literature for POMs@SBA-15 composites (POMs abbreviation for polyoxometalates) [23,27]. These results suggest that the structure of *Aptes*SBA-15 support was intact after HPA immobilization. The porosity of the composite materials was measured through N_2 adsorption-desorption experiments. Both composites exhibited a type IV isotherm with H1 hysteresis loops (Figure S2), characteristic results obtained for mesoporous materials [23,28]. The textural properties of the composites are described in Table 1.

Table 1. Textural properties of the HPAs@*Aptes*SBA-15 composites.

Material	S_{BET} (m^2/g)	V_p (cm^3/g)
H_3PW_{12}@*Aptes*SBA-15	129.07	0.245
H_3PMo_{12}@*Aptes*SBA-15	188.02	0.293

The morphology of the prepared *Aptes*SBA-15 materials was evaluated through SEM analysis (Figure S3), where the characteristic hexagonal elongated particles of the SBA-15 support were observed [23,28]. After HPAs incorporation, it was observed that the morphology of the silica support was maintained (Figure 2). The presence of each HPA in the composite was further confirmed by the presence of the molybdenum and tungsten in EDS analysis (Figure 2).

 doi:10.20944/preprints202403.1537.v1

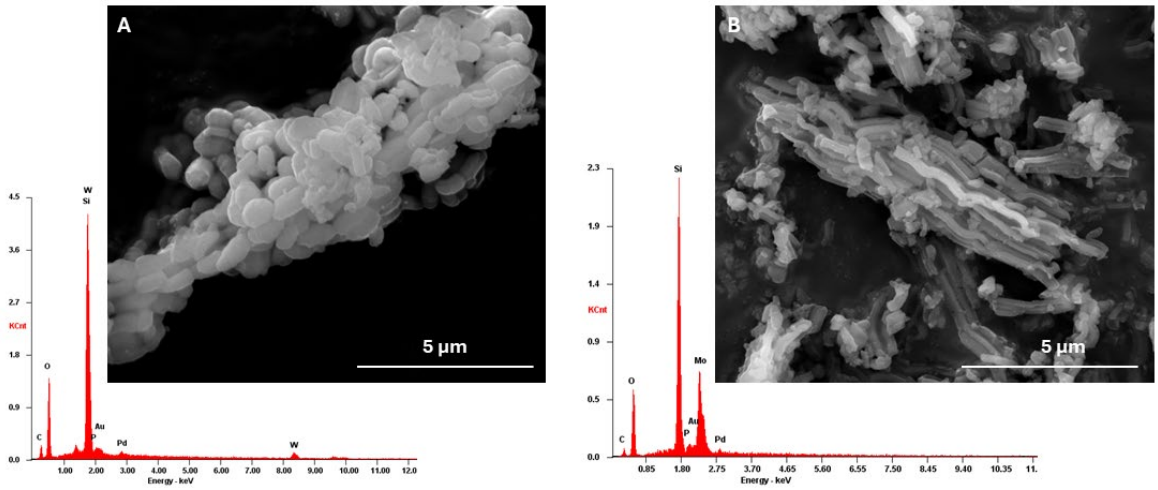

Figure 2. SEM images and EDS spectra obtained for A) H_3PW_{12}@*Aptes*SBA-15 and B) H_3PMo_{12}@*Aptes*SBA-15.

2.2. Acidity Characterization

The acidity present in HPAs and HPAs@*Aptes*SBA-15 composites were evaluated through potentiometric titration, and the results are shown in Table 2. These suggested that the HPAs have higher acidity when compared to the corresponding HPAs@*Aptes*SBA-15 composites. Further, the concentration of released H^+ ions were determined to be 3.36 and 0.47 mmol/g for H_3PMo_{12}@*Aptes*SBA-15 and H_3PW_{12}@*Aptes*SBA-15, respectively.

Table 2. Acidity and pH values for the HPAs and the HPAs@*Aptes*SBA-15 composites.

Material	pH	Acidity (mmol H^+/g)
H_3PMo_{12}	2.2	9.74
H_3PW_{12}	2.2	1.93
H_4SiW_{12}	2.6	0.995
H_3PMo_{12}@*Aptes*SBA-15	3.41	3.36
H_3PW_{12}@*Aptes*SBA-15	3.39	0.470

2.3. Catalytic Activity of HPAs

Previous work developed in the group studied the influence of experimental conditions, in the acetalization reaction of glycerol with acetone, using homogeneous HPAs as catalysts [13]. Optimized results were obtained with a ratio of 1:15 (glycerol/acetone), 3 wt% of HPA (when compared to glycerol weight), and using 25 °C. In this work, the influence of catalyst acidity and molarity was reported, using homogeneous HPAs in the acetalization of glycerol with acetone. Reaction parameters (acetone/glycerol ratio and temperature) were maintained, using the optimized parameters reported previously by Julião et al. [13]. The catalyst acidity of 0.373 mmol H^+/g was used for the different HPAs catalysts (Table 3). The three HPAs (H_3PW_{12}, H_3PMo_{12}, H_4SiW_{12}) were studied at 25 and 60 °C and the results obtained are shown in Figure 3.

 doi:10.20944/preprints202403.1537.v1

Table 3. Normalized acidity and corresponding molarity of the HPA catalysts used.

Material	Acidity (mmol H^+/g)	Catalyst amount (µmol)
H_3PMo_{12}	0.373	0.525
H_3PW_{12}	0.373	1.70
H_4SiW_{12}	0.373	3.26

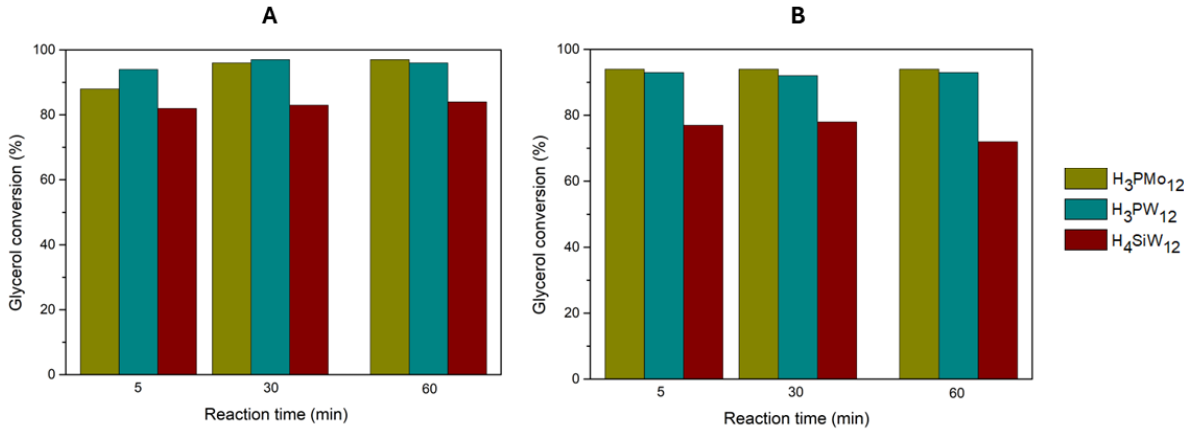

Figure 3. Glycerol conversion results obtained for the three homogeneous catalysts (H_3PMo_{12}, H_3PW_{12} and H_4SiW_{12}), using a ratio of 1:15 glycerol/acetone, a catalyst acidity of 0.373 mmol H^+/g, at **A)** 25 °C and **B)** 60 °C.

At 25 °C, the H_3PW_{12} and H_3PMo_{12} catalysts distinguished themselves, reaching 97% of conversion after 30 and 60 min, respectively. The H_4SiW_{12} exhibited lower conversion, reaching 84% after 60 min. At 60 °C, all three HPAs showed slightly lower conversions than those at 25 °C, with H_3PW_{12} exhibiting the best results (92% conversion after 30 min). Solketal selectivity was above 97% for all catalysts. As such, for the three HPAs, the optimized reaction temperature was 25 °C, as previously reported in the literature [4,13,20]. Therefore, maintaining the acidity of the catalyst, the catalytic activity follows the order: H_3PW_{12} > H_3PMo_{12} > H_4SiW_{12}, with H_3PW_{12}. Previously, our research group performed the same catalytic reactions but maintaining the amount of catalyst (3 wt% of HPA compared to glycerol weight, i.e., 57 µmol of HPA). [13] However, the results obtained for glycerol conversion were identical to the present work, mainly using H_3PW_{12} and H_3PMo_{12} catalysts (Table S4 in SI). With an important advantage in the presence work, since using an acidity normalization of 0.373 mmol H^+/g, much lower amount of catalyst was needed (1.7 µmol of the most active H_3PW_{12} was used, compared to the previous 57 µmol needed previously).

2.4. HPAs@AptesSBA-15 Catalytic Performance

The most active HPAs for the acetalization of glycerol were immobilized in a amine-functionalized *Aptes*SBA-15 support, and the composites (H_3PW_{12}@*Aptes*SBA-15 and H_3PMo_{12}@*Aptes*SBA-15) were used as heterogeneous catalysts. Furthermore, to proceeed a comparison between homogeneous and heterogeneous performance of the most active HPAs, the acidity of the composites was maintained also for 0.373 mmol H^+/g, and the reactions were performed using the same experimental conditions as before for the homogeneous HPAs. The results obtained are displayed in Figure 4, where it was clearly observed that, for both reaction temperatures 25 and 60 °C, H_3PW_{12}@*Aptes*SBA-15 exhibited superior glycerol conversion (83% and 91% after 5 min, respectively) than H_3PMo_{12}@*Aptes*SBA-15 (31% and 40% after 5 min, respectively) composite. Furthermore, H_3PW_{12}@*Aptes*SBA-15 also exhibited the highest solketal selectivity from the two composites, with 97% at both temperatures 25 and 60 °C. Comparing the catalytic results obtained

 doi:10.20944/preprints202403.1537.v1

for the two different temperatures, it is possible to verify that an increase in temperature from 25 to 60 °C resulted only in a slightly better conversion (Figure 4). This indicated that, even at 25 °C, the acetalization reaction of glycerol with acetone, in the presence of HPAs@*Aptes*SBA-15 catalysts, was still a fast-occurring reaction, with the maximum conversion being obtained around 60 minutes.

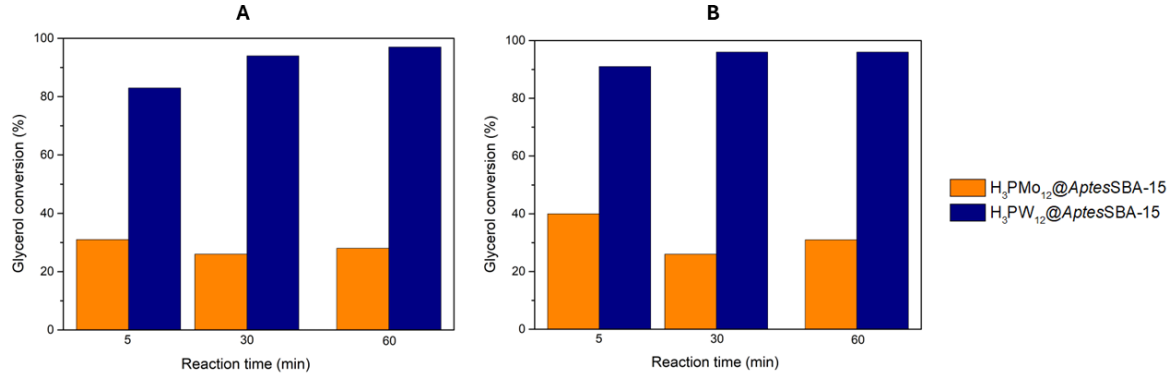

Figure 4. Glycerol conversion results obtained for the two composite catalysts (H_3PMo_{12}@*Aptes*SBA-15 and H_3PW_{12}@*Aptes*SBA-15), using a ratio of 1:15 glycerol/acetone, normalized catalyst acidity of 0.373 mmol H^+/g, at the reaction temperature of **A)** 25 °C and **B)** 60 °C.

To investigate the contribution of the functionalized support *Aptes*SBA-15 in the catalytic activity of the composite, this was used maintaining the catalytic conditions used previously to the composites. However, in this case no catalytic activity was obtained, which confirmed that the acidic sites of the HPAs incorporated in the composite structure are the catalytic active centers and the responsible for the glycerol conversion and the formation of solketal. Such results were previously reported in the literature, being linked to the low acidic behavior of the SBA-15 support [30,31].

3.5. Catalyst Reutilization and Recycling

The best performing heterogeneous catalyst, H_3PW_{12}@*Aptes*SBA-15, was selected for catalyst reutilization tests. The reusability capacity of this catalyst was investigated formin the acetalization reaction of glycerol maintaining the same experimental conditions between various reaction cycles: normalized catalyst acidity of 0.373 mmol H^+/g, a glycerol/acetone ratio of 1:15 and reaction temperature of 25 and 60 °C. Four consecutive reaction cycles where performed and, after each cycle, the reactional solution (unreacted vestigial glycerol, acetone and dissolved products) was removed, and a novel amount of glycerol and acetone were added. The catalyst remained intact, without any treatment between cycles. The reutilization performance of H_3PW_{12}@*Aptes*SBA-15 can be observed in Figure 5, for both 25 and 60 °C. For both temperatures, a decrease in catalyst activity can be observed, particularly after the 2nd cycle. The most accentuated drop-in activity was at 25 °C, with the catalyst demonstrating 28% of glycerol conversion after the 4th cycle, accompanied by a loss in solketal selectivity, from 97% (1st) to 71% (4th). The influence of reaction temperature in the reutilization of HPAs@*Aptes*SBA-15 evaluated at 60 °C showed a smaller loss of catalytic efficiency after the 2nd reaction cycle (69% conversion after the 4th cycle).

 doi:10.20944/preprints202403.1537.v1

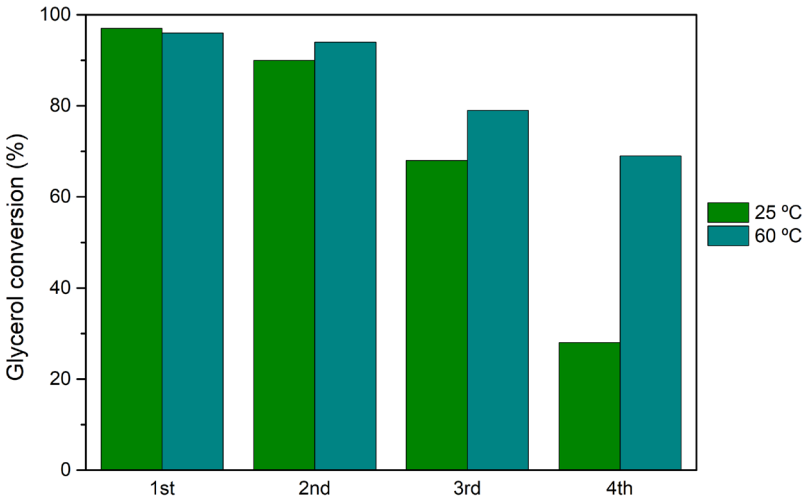

Figure 5. Glycerol conversion results obtained after 1 h of glycerol acetalization with acetone, using H_3PW_{12}@*Aptes*SBA-15 catalyst, after four consecutive reutilization cycles. Reactions performed using a ratio of 1:15 glycerol/acetone, normalized catalyst acidity of 0.373 mmol H^+/g, at the reaction temperature of 25 and 60 °C.

Recycling studies, where the catalyst was washed and activated after each cycle, corroborated with the results obtained previously for the reutilization (without catalyst treatment between cycles), with H_3PW_{12}@*Aptes*SBA-15 demonstrating loss of catalytic activity, at 25 and 60 °C (Figure 6). After the 4th cycle at 25 °C, the catalyst was considered inactive (glycerol conversion of 9%). Using the temperature of 60 °C, smaller loss of catalytic activity was found (54% of conversion, after the 4th cycle).

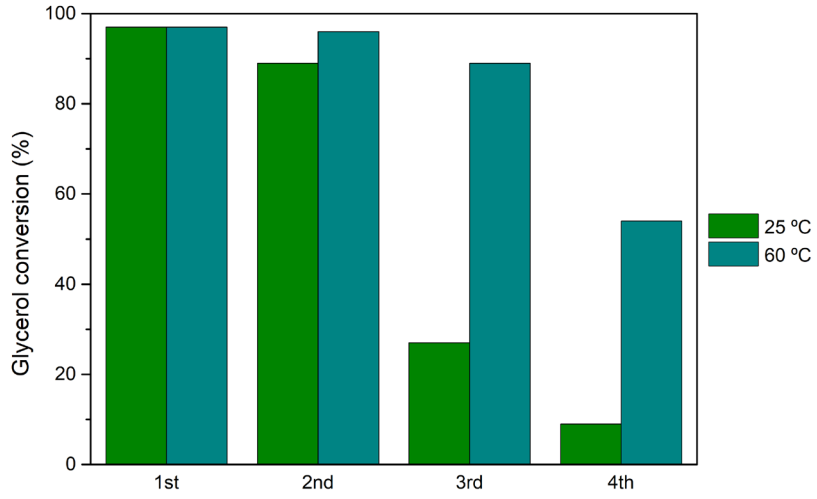

Figure 6. Glycerol conversion results obtained after 1 h of glycerol acetalization with acetone, using H_3PW_{12}@*Aptes*SBA-15 catalyst, after four consecutive recycling cycles. Reactions performed using a ratio of 1:15 glycerol/acetone, normalized catalyst acidity of 0.373 mmol H^+/g, at the reaction temperature of 25 and 60 °C.

The utilization of the H_3PW_{12}@*Aptes*SBA-15 catalyst in consecutive reaction cycles, with or without cleaning treatment between reaction cycles, originated a decrease of glycerol conversion after the 2nd cycle. This is probably due to the catalyst that may suffer a decrease in its acidity after the second consecutive reaction cycle. The loss of acidity can be related to the leaching of the HPAs active sites from the *Aptes*SBA-15 support, a phenomenon reported previously in literature for other catalytic systems [30,32].

 doi:10.20944/preprints202403.1537.v1

3.6. Comparison with Other Catalysts

Some few works can be find in the literature using silica based catalysts in the acetalization of glycerol with acetone, under a solvent-free system (Table 4). In all the reported examples, the selectivity for solketal was higher than 97% and the majority of the reactions were performed at room temperature, highlighting the high suitability of silica-based catalysts for this reaction. Some of these used acid functionalized silica materials, as Vicent et al. that studied the application of sulfonic acid-functionalized silicas [33]. Among the two catalysts, the Ar-SBA-15 exhibited the highest conversion results, with 82.5% of conversion after 0.5 h. Other strategy that has also be applied was the incorporation of different metals in SBA-15 framework. Ammaji et al. obtained high conversions using Nb-SBA-15 catalyst (95% of conversion after 1 h), with 100% of solketal selectivity [31]. However, this catalyst showed a loss of catalytic activity in consecutive reusing reaction cycles. The best performing HPA@silica catalyst was reported by Gadamsetti el al., where the incorporation of molybdenum phosphate into the SBA-15 support resulted in a complete glycerol conversion and very high solketal selectivity (98%) after 1 h of reaction [30]. But also, in this work a loss of active centers and catalytic activity was reported in consecutive reactions. Comparing with the present work and the results obtained with H_3PW_{12}@*Aptes*SBA-15 composite (Table 4), identical results were obtained in shorter reaction time (0.08 h), when the temperature was increased to 60 ºC. In the future experiments, the ratio of glycerol/acetone will be optimized to decrease the amount of acetone used. Under these conditions, the loss of activity during consecutive cycles can be probably avoid or decreased. However, the loss of activity during consecutive reactions is also observed in most of the reported studies using silica-based catalysts for the acetalization of glycerol with acetone.

Table 4. Silica and HPAs@silica composites used as catalysts, in the acetalization of glycerol with acetone, in a solvent-free environment.

Catalyst	Ratio of Glycerol/acetone	T (°C)	Time (h)	Conversion (%)	Selectivity to solketal (%)	*Ref.*
SO_4-Al-MCM-41	1:10	RT	2	94.8	99	[34]
PSF@SiO_2	1:10	RT	1.5	86.6	98	[35]
Ar-SBA-15	1:6	70	0.5	82.5	wi	[33]
Pr-SBA-15	1:6	70	0.5	79.0	wi	[33]
Nb-SBA-15	1:3	RT	1	95	100	[31]
Zr-SBA-15	1:3	RT	1	92	98	[31]
Ti-SBA-15	1:3	RT	1	65	98	[31]
Al-SBA-15	1:3	RT	1	60	98	[31]
MoPo/SBA-15	1:3	RT	1	100	98	[30]
$Cs_{2.5}H_{0.5}PW_{12}O_{40}$@KIT-6	1:6	RT	0.25	95	98	[20]
H_3PW_{12}@*Aptes*SBA-15	1:15	RT 60	0.08	83 91	97 97	This work
H_3PMo_{12}@*Aptes*SBA-15	1:15	RT 60	0.08	31 40	69 76	This work

wi means without information; RT means Room Temperature.

3.7. Catalyst Stability Characterization

After four cycles of recycling, the H_3PW_{12}@*Aptes*SBA-15 catalyst was recovered and characterized by potentiometric titration, ICP-OES, XRD and SEM-EDS. The occurrence of leaching of the HPA and the integrity of the *Aptes*SBA-15 structure were investigated after catalytic use. The heterogeneous catalyst demonstrated a substantial decrease in acidity after the four reaction cycles, what its corroborated with the decrease of the H_3PW_{12} loading after use (Table 5). The XRD pattern of the spent catalyst (Figure S6) exhibited a loss in intensity of the (100) plane, also hindering peak identification for the (110) and (200) planes. SEM imaging demonstrated the occurrence of particle

 doi:10.20944/preprints202403.1537.v1

dispersion, maintaining the characteristic *Aptes*SBA-15 morphology (Figure S7). The presence of H_3PW_{12} was confirmed by the presence of tungsten in the EDS spectra (Figure S7).

Table 5. Acidity characteristics of the H_3PW_{12}@*Aptes*SBA-15 composite, obtained through potentiometric titration and ICP-OES analysis, before use and after its utilization in four catalytic cycles.

H_3PW_{12}@*Aptes*SBA-15	Acidity (mmol H^+/g)	HPA loading (μmol/g)
Before usage	0.469	159
after 4 catalytic cycles	0.277	105

3. Materials and Methods

3.1. Materials

All reagents and solvents used in this work were purchased from commercial sources and used without further purification: Glycerol (99.92%, VWR Chemicals), acetone (99.5%, Honeywell), methanol (99.9%, Fisher Scientific U.K.), Pluronic P123 (Aldrich), hydrochloric acid (HCl, 37%, Aldrich), tetraethoxysilane (TEOS, Aldrich), 3-aminopropyltriethoxysilane (*Aptes*, 98%, Aldrich), anhydrous toluene (99.8 %, Aldrich), acetonitrile (Carlo Reba Reagents), ethanol (99.8%, Honeywell), phosphomolybdic acid hydrate ($H_3[PMo_{12}O_{40}].nH_2O$, Aldrich), phosphotungstic acid hydrate ($H_3[PW_{12}O_{40}].nH_2O$, Aldrich) and silicotungstic acid hydrate ($H_4[SiW_{12}O_{40}].nH_2O$, Aldrich).

3.2. Preparation of Catalysts

The SBA-15 solid support was prepared through a hydrothermal synthesis procedure, adapted from literature [15]. Pluronic P123 (2.0 g) was dissolved in aqueous HCl (2 M, 60 mL) and distilled water (15 mL) under stirring at 40 °C and then TEOS (4.4 g) was added dropwise. The mixture was stirred for 24 h at 40 °C. After cooled, the mixture was transferred to a Teflon autoclave and the temperature raised to 100 °C for another 24 h in. The resulting precipitate was filtered, dried and calcinated at 550 °C for 5 h with a ramp of 1 °C min^{-1}.

The surface of SBA-15 was functionalized via a post-grafting methodology [15]. The SBA-15 support (1 g) was activated for 2 hours at 100 °C, under vacuum. Then, it was dispersed in anhydrous toluene (60 mL) and *Aptes* (0.7 mL). The mixture was placed in a N_2 atmosphere, under constant stirring at 90 °C for 24 h. The resulting material was filtered, washed with toluene and ethanol, and dried under vacuum at 80 °C for 2 h.

The HPAs@*Aptes*SBA-15 composites were prepared through an impregnation technique, adapted from literature [27]. The functionalized support *Aptes*SBA-15 (0.3 g) and acetonitrile (12 mL) were dispersed under constant agitation, at room temperature. Then, the HPA (0.9 g) was added, and the mixture was stirred for 72 hours, at room temperature. The obtained material was filtered, washed with acetonitrile and ethanol, and dried.

3.3. Catalyst Characterization

FTIR-ATR spectra were recorded on a Perkin Elmer Spectrum BX spectrometer, with the ATR operation mode. The spectra were acquired in the 400-4000 cm^{-1} region, with a resolution of 4 cm-1 and 64 scans. All the representations shown in this work present arbitrary units of transmittance. Powder X-ray diffraction (XRD) patterns were collected at room temperature, on a Rigaku's Smartlab diffractometer operating with a Cu radiation source (($\lambda1$ = 1.5405980 Å; $\lambda2$ = 1.5444260 Å; $\lambda2/\lambda1$ = 0.500) and in a Bragg–Brentano θ/2θ configuration (45 kV, 40 mA). XRD analyses were performed in the University of Aveiro – CICECO. Zeta potential measurements were performed at 25 °C, in a Malvern Zetasizer Nano ZS spectrometer. All measurements were repeated three times to verify the reproducibility of the results and samples were prepared by dissolving 1.0 mg of sample in Millipore water (2 mL). Scanning electron microscopy (SEM) and energy dispersive X-ray spectroscopy (EDS)

 doi:10.20944/preprints202403.1537.v1

studies were performed at "Centro de Materiais da Universidade do Porto" (CEMUP, Porto, Portugal) using a FEI Quanta 400 FEG ESEM electron microscope, with a EDAX Genesis X4M energy dispersive X-Ray spectrometer, operating at 15 kV. The samples were studied as powders and were coated with an Au/Pd thin film by sputtering using the SPI Module Sputter Coater equipment. Nitrogen adsorption–desorption isotherms were measured at −186 °C, using an AutoSorb equipment (Quantachrome Instruments, Boynton Beach, FL, USA). Samples were previously evacuated in situ under a high vacuum (10^{-7} bar) for 12 h at 100 °C. The surface area was calculated through the Brunauer–Emmett–Teller (BET) model. The pore volume was obtained using Barret-Joymer-Hallenda (BJH) calculations. HPAs quantification in the composites was possible using a Varian 820-MS spectrometer, through the quantification of molybdenum (Mo) and tungsten (W) present in the materials. Analyses were performed in the University of Santiago de Compostela, Spain. Elemental analysis of C, N and H in *Aptes*SBA-15 was obtained using a Leco CHNS-932 elemental analyzer. Analyses were performed in the University of Santiago de Compostela, Spain. The acidity strength of HPAs and HPAs@AptesSBA-15 materials was obtained through potentiometric titration measurements performed in an TitraLab AT1000 Series instrument, using NaOH (0.025 M) as the base. Solutions of the materials and a NaCl solution were prepared, in a 1:1 ratio, and left at room temperature under stirring, for 24 h. The suspension was separated by filtration.

3.4. Catalytic Experiments

Glycerol acetalization reactions with acetone, under a solvent-free system, proceeded in a closed borosilicate 5 mL catalytic reactor, equipped with a magnetic stirrer, and immersed in a thermostatically controlled liquid paraffin bath. The reactor was filled with the appropriate glycerol/acetone ratio (1:15) and left under agitation with the chosen temperature (25 °C or 60 °C) for 10 min to ensure homogeneity. The catalysts were then added, and the reaction initiated. Reaction progression was evaluated in a Varian CP-3380 gas chromatograph, with a Suprawax-280 capillary column (30 m length, 0.25 mm internal diameter and 0.25 μm film thickness), using H_2 as the carrier gas (flow rate of 55 cm^3/s). At least 3 repeated reactions were performed, and the error obtained was equal or inferior to 5% of conversion of glycerol.

5. Conclusions

The HPA@*Aptes*SBA-15 composites were prepared, characterized, and further used as heterogeneous catalysts for valorization of glycerol thought the acetalization reaction with acetone. The *Aptes*SBA-15 support showed no catalytic activity, owing to its characteristic low acidity. On the contrary, the two prepared composites H_3PW_{12}@*Aptes*SBA-15 and H_3PMo_{12}@*Aptes*SBA-15 showed to be active, mainly when the reaction temperature was increased to 60ºC. The H_3PW_{12}@*Aptes*SBA-15 exhibited superior glycerol conversion (91% after only 5 min and 97% after 60 min, with 97% solketal selectivity). The catalyst was used for four consecutive reaction cycles, with and without the cleaning process of catalysts between reaction cycles. In both cases a loss of catalytic efficiency was observed after the second cycle. The reason of this loss was investigated by performing the characterization of the catalyst after catalytic use during the four consecutive reactions. By acidity and ICP measurements it was possible to identify a leaching of H_3PW_{12} catalytic center. On the other hand, the support materials seem to maintain its structure by using XRD and SEM analysis. Comparing the performance of H_3PW_{12}@*Aptes*SBA-15 with other previously reported in literature, the most prominent advantage of this prepared catalyst is the high yield of solketal that it is possible to obtained after only 5 min of reaction. The weakness of this composite is the stability of H_3PW_{12} in its surface. In the near future different strategies will be adopted to decrease or even eliminate this faintness: decrease the amount of acetone used, functionalize the surface of the silica support with more effective functional groups, and use other structures of silica supports.

Supplementary Materials: The following supporting information can be downloaded at the website of this paper posted on Preprints.org, from Figure S1: title; to Figure S6: title.

 doi:10.20944/preprints202403.1537.v1

Author Contributions: Conceptualization, S.S.B. and F.M.; methodology, C.N.D. and I.S.-V.; validation, S.S.B., F.M. and G. R. G.; investigation, C.N.D.; resources, C. R. G. and S.S.B.; writing—original draft preparation, C.N.D. and F. M.; writing—review and editing, S.S.B. and F.M..; supervision, C.R.G., F.M. and S.S.B.; project administration, F.M. and S.S.B.; funding acquisition, S.S.B. All authors have read and agreed to the published version of the manuscript.

Funding: This work received financial support from *Fundação para a Cinência e a Tecnologia / Ministério da Ciência, Tecnologia e Ensino Superior* (FCT/MCTES) by national funds, through LAQV / REQUIMTE (Ref. UIDP/50006/2020 DOI 10.54499/UIDP/50006/2020; LA/P/0008/2020 DOI 10.54499/LA/P/0008/2020; UIDB/50006/2020 DOI 10.54499/UIDB/50006/2020) and through the CICECO-Aveiro Institute of Materials (UIDB/50011/2020, UIDP/50011/2020 and LA/P/0006/2020).

Data Availability Statement: The data presented in this study are available on request from the corresponding author.

Acknowledgments: : S.S.B. thanks FCT/MCTES for supporting her contract positions via the Individual Call to Scientific Employment Stimulus (Ref. CEECIND/00793/2018 and Ref. CEECIND/03877/2018, respectively). CRG thanks FCT (Foundation for Science and Technology, Portugal) within the scope of UIDB/04423/2020 and UIDP/04423/2020. The position held by I.S.-V. (Ref. 197_97_ARH-2018) was supported by national funds (OE), through FCT, I. P., in the scope of the framework contract foreseen in the numbers 4, 5 and 6 of article 23 of the Decree-Law 57/2016 of 29 August, changed by Law 57/2017 of 19 July.

Conflicts of Interest: The authors declare no conflicts of interest.

References

1. I. Corrêa, R.P.V. Faria, A.E. Rodrigues, Continuous Valorization of Glycerol into Solketal: Recent Advances on Catalysts, Processes, and Industrial Perspectives, Sustainable Chemistry, 2 (2021) 286-324.
2. F. Akram, I.u. Haq, S.I. Raja, A.S. Mir, S.S. Qureshi, A. Aqeel, F.I. Shah, Current trends in biodiesel production technologies and future progressions: A possible displacement of the petro-diesel, Journal of Cleaner Production, 370 (2022).
3. A. Talebian-Kiakalaieh, N.A.S. Amin, N. Najaafi, S. Tarighi, A Review on the Catalytic Acetalization of Bio-renewable Glycerol to Fuel Additives, Front Chem, 6 (2018) 573.
4. M.J. da Silva, M.G. Teixeira, D.M. Chaves, L. Siqueira, An efficient process to synthesize solketal from glycerol over tin (II) silicotungstate catalyst, Fuel, 281 (2020).
5. A. Cornejo, I. Barrio, M. Campoy, J. Lázaro, B. Navarrete, Oxygenated fuel additives from glycerol valorization. Main production pathways and effects on fuel properties and engine performance: A critical review, Renewable and Sustainable Energy Reviews, 79 (2017) 1400-1413.
6. A. Smirnov, S. Selishcheva, V. Yakovlev, Acetalization Catalysts for Synthesis of Valuable Oxygenated Fuel Additives from Glycerol, Catalysts, 8 (2018).
7. I. Fatimah, I. Sahroni, G. Fadillah, M.M. Musawwa, T.M.I. Mahlia, O. Muraza, Glycerol to Solketal for Fuel Additive: Recent Progress in Heterogeneous Catalysts, Energies, 12 (2019).
8. X. Lopez, J.J. Carbo, C. Bo, J.M. Poblet, Structure, properties and reactivity of polyoxometalates: a theoretical perspective, Chem Soc Rev, 41 (2012) 7537-7571.
9. M.N. Timofeeva, Acid catalysis by heteropoly acids, Applied Catalysis A: General, 256 (2003) 19-35.
10. Polyoxometalate Molecular Science, Springer, 2003.
11. D.E. Katsoulis, A Survey of Applications of Polyoxometalates, Chem. Rev., 98 (1998) 359-387.
12. M.J. da Silva, A.A. Julio, F.C.S. Dorigetto, Solvent-free heteropolyacid-catalyzed glycerol ketalization at room temperature, RSC Advances, 5 (2015) 44499-44506.
13. D. Juliao, F. Mirante, S.S. Balula, Easy and Fast Production of Solketal from Glycerol Acetalization via Heteropolyacids, Molecules, 27 (2022).
14. I.V. Kozhevnikov, Catalysis by Heteropoly Acids and Multicomponent Polyoxometalates in Liquid-Phase Reactions, Chem. Rev., 98 (1998) 171-198.
15. S.O. Ribeiro, C.M. Granadeiro, P.L. Almeida, J. Pires, M.C. Capel-Sanchez, J.M. Campos-Martin, S. Gago, B. de Castro, S.S. Balula, Oxidative desulfurization strategies using Keggin-type polyoxometalate catalysts: Biphasic versus solvent-free systems, Catalysis Today, 333 (2019) 226-236.
16. J. Li, Z. Yang, G. Hu, J. Zhao, Heteropolyacid supported MOF fibers for oxidative desulfurization of fuel, Chemical Engineering Journal, 388 (2020).
17. P. Ferreira, I.M. Fonseca, A.M. Ramos, J. Vital, J.E. Castanheiro, Acetylation of glycerol over heteropolyacids supported on activated carbon, Catalysis Communications, 12 (2011) 573-576.
18. J.E. Castanheiro, J. Vital, I.M. Fonseca, A.M. Ramos, Glycerol conversion into biofuel additives by acetalization with pentanal over heteropolyacids immobilized on zeolites, Catalysis Today, 346 (2020) 76-80.

 doi:10.20944/preprints202403.1537.v1

19. P. Verma, Y. Kuwahara, K. Mori, R. Raja, H. Yamashita, Functionalized mesoporous SBA-15 silica: recent trends and catalytic applications, Nanoscale, 12 (2020) 11333-11363.
20. L. Chen, B. Nohair, D. Zhao, S. Kaliaguine, Highly Efficient Glycerol Acetalization over Supported Heteropoly Acid Catalysts, ChemCatChem, 10 (2018) 1918-1925.
21. J. Castanheiro, Acetalization of Glycerol with Citral over Heteropolyacids Immobilized on KIT-6, Catalysts, 12 (2022).
22. J. Goscianska, A. Olejnik, I. Nowak, APTES-functionalized mesoporous silica as a vehicle for antipyrine – adsorption and release studies, Colloids and Surfaces A: Physicochemical and Engineering Aspects, 533 (2017) 187-196.
23. F. Mirante, N. Gomes, L.C. Branco, L. Cunha-Silva, P.L. Almeida, M. Pillinger, S. Gago, C.M. Granadeiro, S.S. Balula, Mesoporous nanosilica-supported polyoxomolybdate as catalysts for sustainable desulfurization, Microporous and Mesoporous Materials, 275 (2019) 163-171.
24. A.S.M. Chong, X.S. Zhao, Functionalization of SBA-15 with APTES and Characterization of Functionalized Materials, J. Phys. Chem. B, 107 (2003) 12650-12657.
25. A. Aouissi, Z.A. Al-Othman, H. Al-Anezi, Reactivity of heteropolymolybdates and heteropolytungstates in the cationic polymerization of styrene, Molecules, 15 (2010) 3319-3328.
26. J. Pires, S. Borges, A. Carvalho, C. Pereira, A.M. Pereira, C. Fernandes, J.P. Araújo, C. Freire, Magnetically recyclable mesoporous iron oxide–silica materials for the degradation of acetaminophen in water under mild conditions, Polyhedron, 106 (2016) 125-131.
27. F. Mirante, S.O. Ribeiro, B. de Castro, C.M. Granadeiro, S.S. Balula, Sustainable Desulfurization Processes Catalyzed by Titanium-Polyoxometalate@TM-SBA-15, Topics in Catalysis, 60 (2017) 1140-1150.
28. Sujandi, S.E. Park, D.S. Han, S.C. Han, M.J. Jin, T. Ohsuna, Amino-functionalized SBA-15 type mesoporous silica having nanostructured hexagonal platelet morphology, Chem Commun (Camb), (2006) 4131-4133.
29. C.M.P.-M. Craig L.Hill, Homogeneous catalysis by transition metal oxygen anion clusters, Coordination Chemistry Reviews, 143 (1995) 407-455.
30. S. Gadamsetti, N.P. Rajan, G.S. Rao, K. V. R. Chary, Acetalization of glycerol with acetone to bio fuel additives over supported molybdenum phosphate catalysts, Journal of Molecular Catalysis A: Chemical, 410 (2015) 49-57.
31. S. Ammaji, G.S. Rao, K.V.R. Chary, Acetalization of glycerol with acetone over various metal-modified SBA-15 catalysts, Applied Petrochemical Research, 8 (2018) 107-118.
32. L. Chen, B. Nohair, D. Zhao, S. Kaliaguine, Glycerol acetalization with formaldehyde using heteropolyacid salts supported on mesostructured silica, Applied Catalysis A: General, 549 (2018) 207-215.
33. G. Vicente, J.A. Melero, G. Morales, M. Paniagua, E. Martín, Acetalisation of bio-glycerol with acetone to produce solketal over sulfonic mesostructured silicas, Green Chemistry, 12 (2010).
34. B. Matkala, S. Boggala, S. Basavaraju, V.S. Sarma Akella, H.P. Aytam, Influence of sulphonation on Al-MCM-41 catalyst for effective bio-glycerol conversion to Solketal, Microporous and Mesoporous Materials, 363 (2024).
35. R. Zhou, Y. Jiang, H. Zhao, B. Ye, L. Wang, Z. Hou, Synthesis of solketal from glycerol over modified SiO2 supported p-phenolsulfonic acid catalyst, Fuel, 291 (2021).